

The exosystems around HD 169830 and HD 12661: are they dynamical twins?

Krzysztof Goździewski¹

Toruń Centre for Astronomy, N. Copernicus University, Gagarina 11, 87-100 Toruń, Poland

Maciej Konacki²

*Department of Geological and Planetary Sciences, California Institute of Technology, MS 150-21,
Pasadena, CA 91125, USA*

Nicolaus Copernicus Astronomical Center, Polish Academy of Sciences, Rabiańska 8, 87-100 Toruń, Poland

ABSTRACT

The new 2-planetary system around HD 169830 has been announced during the XIX-th IAP Colloquium "Extrasolar Planets: Today & Tomorrow" (Paris, June 30 - July 4, 2003) by the Geneva Extrasolar Planet Search team. We study the orbital dynamics of this system in the framework of the N -body problem. The analysis of its orbital stability is performed using the long-term integrations and the fast indicators, the Mean Exponential Growth factor of Nearby Orbits and the Frequency Map Analysis. The HD 169830 appears to be located in a wide stable region of the phase space. The ratio of the mean motions of the planets HD 169830 b and c is between low-order mean motion resonances, 9:1 and 10:1. The long-term integration of the coplanar configurations, conducted over 1 Gyr, reveals that the eccentricities of the companions vary with a large amplitude $\simeq 0.4 - 0.5$ but there is no sign of instability. The orbital parameters of the planets resemble those of another 2-planetary system, around HD 12661. Both of them can be classified as hierarchical planetary systems. We investigate whether these two exosystems are dynamically similar. Such similarities may be important for finding out if the formation and subsequent orbital evolution of exoplanetary systems obey common rules.

Subject headings: celestial mechanics, stellar dynamics—methods: numerical, N-body simulations—planetary systems—stars: individual (HD 169830, HD 12661)

1. Introduction

The radial velocity survey for extrasolar planetary systems conducted by the Geneva Extrasolar Planet Search Team has recently revealed a new planetary system around HD 169830. This discovery has been announced during the XIX-th IAP Colloquium "Extrasolar Planets: Today & Tomorrow", (Paris, June 30 - July 4, 2003). In this paper we perform a preliminary analysis of the orbital stability of the HD 169830 system and its dependence on the orbital parameters that are unconstrained by radial velocity (RV) observations. In the numerical experiments, we use two sets of the orbital parameters from the 2-Keplerian fits to the RV measurements. The first set was published by the authors on their web site in June 2003³ and the second,

¹e-mail: k.gozdziewski@astri.uni.torun.pl

²e-mail: maciej@gps.caltech.edu

³http://obswww.unige.ch/udry/planet/hd169830_syst.html

most recent set is from Mayor et al. (2003). Our early analysis of the first set of the orbital elements revealed a curious, close similarity to the orbital elements of the HD 12661 system (Fischer et al. 2003; Goździewski & Maciejewski 2003). These two hierarchical planetary systems (HPS) appeared to have very similar ratios of the minimal masses $\mu = m_b/m_c \simeq 1.3$, the semi-major axes $\alpha = a_b/a_c \simeq 0.3$ and similar initial eccentricity of the outer planet $e_c \simeq 0.3$ with simultaneously small eccentricity of the inner planet $e_b \simeq 0$. As we show in this paper, in such a case both systems would be located in a large island of the secular apsidal resonance with the semi-major axes antialigned in the exact resonance. There could be another planetary system, around HD 160691 (Jones et al. 2002), with a qualitatively similar dynamics as suggested by Goździewski et al. (2003). In a relatively small number of about 14 multi-planetary systems known to the date⁴, these three cases of supposedly identical configuration inspired us to ask whether such a dynamical resemblance can be casual or has a deeper origin in their formation scenario and/or orbital evolution.

However recently, the Geneva team has published a new orbital solution substantially different than the first one (see Mayor et al. 2003). In the new solution the elements of the outer companion are dramatically altered. The period and the semi-major axis of the outer planet are changed by $\simeq 600$ d and $\simeq 0.7$ AU respectively. This obviously leads to a qualitatively different orbital configuration than the one analyzed before. The proximity of the HD 169830 and HD 12661 systems does not seem to be so clear anymore. Still, the orbital elements of the inner companions appear to be almost identical in the two planetary systems. Because the observational window of HD 169830 covers only about 1 orbital period of the outer planet, its orbital elements are still not well constrained. In our numerical experiments, we use both solutions although the old one essentially for a reference and an interesting comparison with the predictions given by the secular octupole-level theory (Lee & Peale 2003).

According to Lee & Peale (2003), one has to employ a proper representation of the orbital fits to the RV observations, particularly in the case of the HPS. The orbital fits to the RV of HPS are best interpreted in Jacobi coordinates and these coordinates should be used in the dynamical investigations. Specifically, the authors demonstrate that the orbital time-evolution when expressed in the commonly used astrometric elements can lead to spurious effects like a large scatter of the osculating semi-major axis and eccentricity of the outer planet about the secular value or a significant dependence of the integration results on the initial epoch. Unfortunately, the RV measurements of the HD 169830 system have not been published to the date. However, assuming that the best-fit parameters K, n, e, ω, T_p (where, for every planet involved, K is the semi-amplitude of RV variations, n is the mean motion, e is the eccentricity, ω is the periastron argument and T_p is the time of periastron passage) describe a 2-Keplerian fit, they represent in fact the orbital parameters in the Jacobi coordinate system (Lee & Peale 2003) and using them, we can recover the semi-major axes a and the minimal masses of the companions. In some of the numerical experiments carried out in this paper, the inclination of the outer planet was changed by a tiny value, to 89.9° , to allow the system enter the third spatial dimension for the purpose of the numerical integrations. The periastron passage of the inner planet is selected as the initial epoch of the osculating elements inferred from the 2-Keplerian solutions. The two ICs used in the computations are given in Table 1. The first, preliminary one, IC is labeled by ICI and the current one by ICII. In some experiments we modified ICI, by setting $e_c \simeq 10^{-6}$, to avoid numerical singularities. The elements of the HD 12661 system are given in Table 3 and we refer to them as IC0 throughout this work.

⁴<http://www.encyclopaedia.fr>

2. Numerical setup

We use the so-called fast indicators, MEGNO and FMA as the main numerical tools to study the orbital stability of the HD 169830 system. The indicator called MEGNO (the Mean Exponential Growth Factor of Nearby Orbits), has been invented by Cincotta & Simó (2000) and we have applied it in the studies of the exosystems’ dynamics described in a series of recent papers (for details and references on MEGNO see, for example, Goździewski et al. 2001; Goździewski & Maciejewski 2003). The MEGNO is a very efficient tool—typically, it makes it possible to distinguish between regular and chaotic dynamics during an integration of the system carried out over $\simeq 10^4$ orbital periods of the outermost planet. This indicator provides a direct estimate of the stability in the strict sense of the maximal Lyapunov Characteristic Number (LCN). As in the previous works, the MEGNO integrations are driven by a Bulirsh-Stoer integrator, namely the ODEX code (Hairer & Wanner 1995). The relative and absolute accuracies of the integrator are set to 10^{-14} and $5 \cdot 10^{-16}$, respectively. The zones of stability, corresponding to quasiperiodic motions of the system, are marked in the MEGNO maps by values close to 2. The positions of the nominal conditions are marked in the contour plots by the intersection of the two thin lines. In this work, we make yet another use of the integrations. During the MEGNO integrations we simultaneously analyze the osculating elements to study the short-term dynamics of the system. The osculating orbital elements feed the Frequency Map Analysis (FMA) algorithm (Laskar 1993). The FMA, an already classic fast indicator, allows us to detect orbital resonances and determine diffusion rates of the fundamental frequencies in the planetary system (Robutel & Laskar 2001). The diffusion rate is a quantity that cannot be determined by the LCN, however it also measures the lack of regularity of an orbit. Along a quasi-periodic solution the fundamental frequencies are constant. For a chaotic orbit these frequencies change and by calculating their diffusion rates, one can directly detect the macroscopic changes of the orbital elements. Thus by combining both methods, it is possible to derive extensive information on the system’s dynamics.

Since our computations concern mostly a short-term dynamics of the planetary system, the FMA is very useful in identifying the positions of the mean motion resonances (MMRs). In order to identify these resonances, during every integration of MEGNO, the complex functions $f_k(t_i) = a_k \exp i\lambda_k(t_i)$ are computed for planets $k = b, c$ at the discrete times t_i , where $t_{i+1} - t_i < 0.5P_b$, over the time $2T$ of the order of $10^4 P_c$ ($P_{b,c}$ are the orbital periods of the inner and outer companion, respectively). Here, a_k denotes the semi-major axis and λ_k is the mean longitude of the planet. If the motion is quasiperiodic then in the time series $\{f_k(t_i)\}$, the frequency ν_k corresponding to the largest amplitude a_k^0 is one of the fundamental orbital frequencies of the system, called the proper mean motion, n_k (Robutel & Laskar 2001). Because the secular frequencies are much smaller than the orbital frequencies, in the first approximation the precession of the orbits can be neglected and MMRs can be identified through the condition $q\nu_b - p\nu_c \simeq 0$, where $p, q > 0$ are prime integers. The FMA gives the ratios $\nu_b/\nu_c \simeq p/q$, and then p and q can be easily resolved by the continued fraction algorithm.

After finding $\nu_{b,c}^{(1)}$ and $\nu_{b,c}^{(2)}$ where $\nu_{b,c}^{(1,2)}$ are the proper mean motions $n_{b,c}$ obtained after integrating the system over the time intervals $[0, T]$, and $[T, 2T]$, respectively, the diffusion rate is determined through $\sigma_k = 1 - \nu_k^{(2)}/\nu_k^{(1)}$ (Robutel & Laskar 2001). Following these authors, if the motion is quasiperiodic, σ_k is equal to zero or, computed with the FMA algorithm, is a very small quantity, typically less than $\simeq 10^{-8}$ while for an irregular chaotic motion, σ_k is larger by several orders of magnitude. The inferred diffusion of the semi-major axis, can be derived through the Kepler law $n^2 a^3 = \mu$ as $\Delta n/n \simeq -3/2(\Delta a/a)$. In this way, although the time span of the integrations is relatively very short, the most relevant instabilities of the motion can be detected and identified.

In this paper, we use the FMA code kindly provided by David Nesvorný on his web page⁵. According to the author, the code incorporates the idea of the Frequency Modified Fourier Transform, FMFT (Sidlichovsky & Nesvorný 1997). We use a variant of the FMFT, with the so-called additional non-linear correction (see the cited paper for details). We have tested this code to make sure that it resolves the mean motions of non-interacting (Keplerian) orbits with the accuracy consistent with the internal precision of the method (set to 10^{-10}).

3. Orbital fits

The two distinctively different orbital solutions, ICI and ICII, announced within a short period of time by the Geneva group strongly suggest that at least one of them corresponds to a local minimum of $(\chi^2_\nu)^{1/2}$. Unfortunately, it is not possible to verify their elements since the RV measurements are not available. In order to get at least some insight into the reliability of the newest set of orbital parameters, we have digitized the figure with RV measurements published on their WWW site⁶. The 93 data points we obtained differ from the real observations (for example, it is difficult to recover the exact moments of the observations), but they still properly describes the overall shape of the observed RV curve and its characteristic features. Note also that our set of "measurements"⁷ is smaller than the real one (112) because in some parts of the RV curve it was very difficult to clearly resolve all points due to a dense sampling of the real measurements. We assume that the observational errors are given by $\sigma = \sigma_0 + \sigma_1$ where $\sigma_0 = 8.5$ m/s and σ_1 is an artificial normal random noise of 0 mean and the standard deviation about 1, resulting in the "errors" in the range [6, 11] m/s and roughly approximating the scale of the real errors.

We used the genetic algorithm scheme (GA) implemented by Charbonneau (1995) in his publicly available⁸ code PIKAIA to to look for a global, coplanar orbital solution. The data were modeled with 2-Keplerian model (as in Goździewski et al. 2003) and the self-consistent Newtonian model, i.e., driven by the full N -body dynamics (Laughlin & Chambers 2001). For the first model the GA code was executed a few hundreds of times and repeatedly found a solution very close to the best one, given in Table 2. Even though the number of our "measurements" is smaller than in the real set, the similarity of the orbital solutions is very significant. Remarkably, the GA found very similar parameters for the outer planet (although the differences are larger than for the inner planet). The best fit parameters have the $(\chi^2_\nu)^{1/2} \simeq 1.21$ and the rms of $\simeq 10$ m/s. This experiment was also repeated for two other data sets with 104 and 105 points (from two slightly different digitization) with the errors in the range [5, 12] m/s and [7, 10] m/s, respectively. The obtained best fit solutions were qualitatively the same as those given in Table 2 (let us note that the differences were most significant for $e_b \simeq 0.29$, $e_c \simeq 0.29$ and $\omega_c \simeq 270^\circ$). Our analysis indicates that the ICII by the Geneva group is really close to the global minimum of $(\chi^2_\nu)^{1/2}$ and should not change at least if based on the currently available set of the RVs.

With the second model that accounts for the mutual interactions between planets, the best fit solution is not significantly better. It is characterized by the $(\chi^2_\nu)^{1/2} \simeq 1.21$ and the rms of $\simeq 9.5$ m/s. The corresponding orbital parameters are very similar to those from the 2-Keplerian fit (see Table 2; for a

⁵<http://www.boulder.swri.edu/~davidn/fmft/fmft.html>

⁶http://obswww.unige.ch/~udry/planet/hd169830_syst.html

⁷The set is available upon request from KG

⁸<http://www.hao.ucar.edu/public/research/si/pikaia/pikaia.html>

reference, the synthetic RV-curves and the digitized "data" points are also shown in Fig. 4). This result suggests that the current RV set does not allow to detect significant N -body coupling (for example, from low-order resonances). Finally, to roughly estimate the formal errors of the self-consistent Newtonian fit, we determined the confidence intervals of $(\chi_\nu^2)^{1/2}$ (Press et al. 1992). The results are illustrated in Fig. 5. Clearly, the formal errors of a_c and e_c (semi-major axis and eccentricity of the outer planet) are substantial but the minimum of $(\chi_\nu^2)^{1/2}$ is well localized. We note that to estimate the conservative errors in the best-fit parameters, the effect of stellar "jitter" should be taken into account (as in Goździewski & Maciejewski 2003).

4. Orbital stability of the HD 169830 system

Both orbital configurations of HD 169830, ICI and ICII, appear to be stable. The evolution of the Jacobi osculating orbital elements computed over the time span of $\simeq 3.6 \cdot 10^4$ revolutions of the outer planet (about 150,000 yr) for the ICI fit is illustrated in Fig. 1. During this time, the eccentricities (see Fig. 1c) vary with a large full-amplitude of about 0.35. Fig. 1d reveals a presence of the secular apsidal resonance (SAR) in which the apsides are on the average antialigned. The semi-amplitude of the librations, θ (where $\theta = \varpi_b - \varpi_c$ and $\varpi_{b,c}$ are the respective longitudes of periastron), is about 90° . Apparently, the orbital elements vary in a regular way and this is strictly confirmed by the MEGNO signatures. The temporal changes of MEGNO, $Y(t)$, are shown in Fig. 1e and its mean value, $\langle Y \rangle(t)$ (Fig. 1f), perfectly converges to 2. For a comparison, we computed these quantities for the HD 12661 system using the IC0 from Table 3. The results are shown in Figure 3. In both these cases, the variations of the orbital elements and the character of MEGNO convergence are qualitatively identical. However, the ICII fit for the HD 169830 system results in a qualitatively different orbital evolution (Fig. 2). The SAR does not seem to be present anymore. Nevertheless, the MEGNO signature (computed over about 550,000 yr) indicates a stable, quasiperiodic configuration.

The MEGNO signatures have been verified by direct 1 Gyr integrations using the RMVS3 integrator from the SWIFT package (Levison & Duncan 1994). We repeated the integrations with two different time steps, equal to 8 and 10 days. As one would expect, no instability occurs during this time and the orbital elements vary within the bounds determined by the short-term integrations. We do not show these results as they are basically an extension of the plots shown in Figures 1, 2 and 3. Obviously, due to the uncertainties of the orbital fits, such an examination of the isolated IC's is not representative for the system's dynamics. In order to find out whether the dynamics is robust to small adjustments of the initial condition, we have computed one-dimensional scans of $\langle Y \rangle$ by changing the semi-major axis of the outer planet and keeping the other orbital parameters fixed at their initial values given in Table 1 for HD 169830 and 3 for HD 12661. The results of this experiment are shown in Fig. 6. The MEGNO scan (the upper graphs of the respective panels in Fig. 6), computed with the resolution of about $3 \cdot 10^{-4}$ AU, reveals a number of spikes. Most of these spikes represent the MMRs between the planets. This identification is based on the FMA as described in the previous Section. We marked MMRs of the order $p + q$ not greater than about 20. These scans reveal that the dynamical environment of the nominal ICs is qualitatively the same for the ICI of the HD 169830 and the IC0 of HD 12661 systems. The outer planet lies in a stable zone between strong MMRs 6:1 and 7:1. The graph for the ICII of the HD 169830 system reveals a different dynamical environment. Clearly, the change in e_c (compared to e_c from ICI) "shifted" the system to the zone between the 9:1 and 10:1 MMRs.

The FMA working with the MEGNO code enabled us to find out how sensitive both methods are to the instabilities of the motion. Bottom parts of the panels of Fig. 6 show the diffusion rate computed for

the outer planet and estimated over its $\simeq 18,000$ orbital periods. In the regions of quasiperiodic motions, as classified by MEGNO, the diffusion rate, σ_c , is smaller than about 10^{-8} . Such small values ensure us that the motion is close to a quasiperiodic evolution. In the MMRs zones σ_c grows up to $10^{-2} - 10^{-1}$. Hence in these areas, the osculating orbital elements exhibit macroscopic changes. Both algorithms are in an excellent accord, as they provide the same positions of the MMRS and very similar estimates of their widths. In other experiments, we noticed that for much shorter integration times, $\simeq 0.45 \cdot 10^4 P_c$, both algorithms can still detect all the relevant MMRs although in this case they do not allow to point out clearly enough some of the weak resonances. In fact, for the four times longer integration ($\simeq 1.8 \cdot 10^4 P_c$), the FMA seems to be even more sensitive to the presence of weak resonances than the MEGNO algorithm is. We note here that by a compromise forced by the numerical efficiency of the code, in further runs of MEGNO, we have set the integration time to about $0.9 \cdot 10^4 P_c$.

5. Global dynamics of the HD 169830 system

To extend the above one-dimensional analysis, we can investigate the stability of the HD 169830 system in a few representative planes of its orbital parameters.

The program computing MEGNO simultaneously evaluated the maximal values of the eccentricities, $e_{b,c}^{\max}$, attained during the integration time. We also stored the maximal value of semi-amplitude of the librations, θ^{\max} , after every step (set to P_c) of renormalization of the variational equations. It helped us to detect the apsidal resonance and to estimate the semi-amplitude of the librations. The maximal value of the critical argument θ was taken relative to the center of the libration 0° or 180° . To avoid the effects of a possible transition into the SAR, the determination of θ^{\max} was started after the first half of the integration period (about $0.45 \cdot 10^4 P_c$). Finally, if $\theta^{\max} < 90^\circ$, then we treated this value as a semi-amplitude of the apsidal librations. The period of the integrations is relatively short but as we show in Goździewski (2003), such information on the short-term dynamics can still give us much insight into the global behaviour of the system. The results are illustrated in Figs. 7–9, where the left panels are for MEGNO, $\langle Y \rangle$, the middle panels are for θ^{\max} and the right panels are for e_b^{\max} . In these scans, the initial parameters that are varied are the coordinates of the maps and the other initial orbital elements are fixed at their nominal values given in Table 1.

Figure 7 is for the (a_c, e_c) -plane. Since the resolution of these maps is 200×50 data points and the integration time is shorter than that of the one-dimensional a_c scan (shown in Fig. 6), there is a lack of some fine resonance structures visible in Fig. 6. Yet the location of the dominant low-order MMRs: 6:1, 13:2 and 7:1 for ICI and 8:1, 9:1 and 10:1 for ICII, as well as their widths are clearly marked. The system would be chaotic for e_c roughly greater than 0.5-0.6. In the central, stable parts of the MMRs, the maximal values of e_b are small indicating their stabilizing influence on the motion. For ICI of the system around HD 169830 (as well as for IC0 of the HD 12661 system, not shown here), the plot for θ^{\max} reveals an extended zone of the SAR about the libration center of 180° . For very small initial $e_c \simeq 0$, the semi-amplitude of librations reaches the limiting 90° . If the eccentricity becomes larger than $\simeq 0.005$ then the semi-amplitude decreases rapidly to 60° - 70° . The same type of (a_c, e_c) -scans of MEGNO for the HD 12661 system is shown in Goździewski (2003) (his Fig. 6) and Goździewski & Maciejewski (2003) (their Fig. 3). In both cases, the MEGNO structures around the nominal ICs are very similar. Interestingly, the (a_c, e_c) -maps of MEGNO for some of the fits to the RV data of the HD 160691 planetary system in Goździewski et al. (2003) (e.g., the fits GM5 and GM6, Fig. 5 in that paper), describe a dynamical setup very similar to these of the HD 169830 (with ICI) and HD 12661 systems. This is no longer true for the ICII of the HD 169830 system. In this

case, the zone of the SAR is confined to a very small e_c (but over wide range of a_c) and to the centers of the MMRs (see Fig. 7, bottom panels).

Figure 8 shows the behaviour of MEGNO, the semi-amplitude of apsidal libration and the maximal eccentricity of the inner planet for HD 169830 system on the (e_b, e_c) -plane. The nominal configuration of the system (denoted as previously by the intersection of the two thin lines) is located in an extended zone of quasiperiodic motions as seen in the MEGNO map (Fig. 8, panels in the left column). The e_b^{\max} -maps (Fig. 8, right column) enable us to determine the border of the global instability established by these values of the initial e_c which lead to large maximal eccentricities. For ICI, this border is substantially shifted towards larger initial eccentricities compared to the border of chaotic zone visible in the MEGNO map but overall it has a similar shape. The same effects are seen for ICII. In the SAR-maps (Fig. 8, middle column), for both IC's one can find a very sharp border of this resonance in the region of small e_b . For ICI, it ends at the border of unstable motion present in the relevant e_b^{\max} panel. For ICII, the semi-amplitude of the librations is about 60° – 70° in this area but as for ICI (Fig. 7, middle panel), a very narrow strip of semi-amplitudes of $\sim 90^\circ$ for the initial $e_c \simeq 0$ is present. These large-amplitude librations for small e_c are explained in the next section. Let us note that also in this test, the obtained picture of the stability zones for ICI of the HD 169830 system is qualitatively the same as for the HD 12661 system — see Fig. 5 and the discussion from Goździewski (2003). However, the SAR-map is quite different for ICII since the SAR is confined to a narrow zone of regular motion about small initial e_c and also to unstable zone which is seen around $(e_b, e_c) = (0.47, 0.47)$.

In the next set of experiments, we determine the zones of stability while the system inclination and hence planetary masses are varied. Assuming that the (unknown) inclinations of the orbits are the same $i = i_b = i_c$, the relative inclination i_{rel} of the orbits depends on the difference of the nodal longitudes, $\Delta\Omega = \Omega_c - \Omega_b$, according to the formula:

$$\cos(i_{\text{rel}}) = \cos(i_b) \cos(i_c) + \sin(i_b) \sin(i_c) \cos \Delta\Omega.$$

We assume that both orbits are prograde. By changing i , the masses are altered because the minimum masses, $m_{b,c} \sin i$, corresponding to edge-on orbits, must be preserved.

The results are shown in Fig. 9. For both ICI and ICII, even for large relative inclinations, the zones of stability extend up to very low system inclinations, $i \simeq 15^\circ$. This is supported by the e_b^{\max} -scan which is shown in the right panel of this figure. In some unstable zones, seen in the MEGNO map for the ICI (Fig. 9, top-left panel), we can identify the 13:2 MMR. It quickly destabilizes the system in the areas about $i \simeq 45^\circ$ — in these regions both eccentricities increases rapidly up to 0.8–0.9. In the strip about low inclinations, most likely thanks to the SAR, this effect is absent.

For ICI, due to the initial $e_c \simeq 0$ and a geometrical singularity (for very small eccentricity the argument of periastron becomes undefined), our numerically computed θ^{\max} -map (top-middle panel of Fig. 9) does not allow to clearly detect the zone of the SAR. However, in our preliminary study of the ICI we set $e_c \simeq 0.007$ and then we found a wide zone of the SAR in the central part of the scanned area. The overall picture is qualitatively the same as in the case of the HD 12661 system (Goździewski & Maciejewski 2003) where for low- i_{rel} configurations, the SAR persists almost in the entire range of the system inclination i .

For ICII, the unstable zones in the MEGNO map are basically similar to those of the ICI of the HD 169830 and HD 12661 systems. Interestingly, all the maps for maximal e_b reveal characteristic quarter-circle areas in which the eccentricity grows up to 1. In the strips near the central parts and corresponding to $e_b \simeq 1$ the configuration becomes chaotic (compare the MEGNO- and e_b^{\max} -maps). The analysis of the orbits

in these areas shows that together with the excitation of the inner planet’s eccentricity, the inclination of this planet oscillates with a very large amplitude. It is illustrated in Figure 10 for the ICII and the initial relative inclination set to 80° . Let us observe that in this case e_b approaches 0.9 while the inclination goes up to 140° . Nevertheless, the system still remains rigorously stable. This phenomenon seems to be an analogue of the Kozai resonance (Kozai 1962) that is known for highly inclined asteroids and generally has been observed in triple systems in which the mass of the inner body is much smaller than the mass of the central and the outer body (Holman et al. 1997). In the multi-planetary exosystems, the masses of the perturber and the inner body are comparable which makes the problem more complex than in the asteroidal approximation. Let us note that a possibility of this phenomenon has been analyzed in ν Andromedae case (Chiang et al. 2001). The inclined configurations which we study here are rather special because it has been assumed that the initial inclinations are the same for both planets. However, a similar behaviour can be expected when the absolute inclinations are varied independently. It has been observed also in other hierarchical exosystems (see for example Goździewski 2003; Goździewski 2003). Since this phenomenon provides strong dynamical limits on the relative inclinations, it certainly deserves a detailed study which we plan to carry out in a future paper.

6. Secular apsidal resonance

The SAR in the HD 12661 exosystem was analyzed numerically in Goździewski (2003). We found an extended zone of the SAR in wide ranges of the semi-major axes, eccentricities and masses of the companions. Similar behavior of the SAR can be observed for the ICI of the HD 169830 system. It should be noted that those results were based on the IC of the HD 12661 system derived from the 2-Keplerian model by Fischer et al. (2003). Our attempts to analyze the same RV data set resulted in a rather different orbital solution (Goździewski & Maciejewski 2003). Yet, the overall SAR features did not change. These results have been confirmed and greatly extended analytically by Lee & Peale (2003) in the framework of their octopole-level secular planetary theory.

Here, we literally quote that basics of their theory, which are relevant for our further analysis. This theory describes the secular dynamics in a coplanar hierarchical 2-planet system. It is assumed that MMRs are absent. The equations of motion originate from the Hamiltonian which is expanded up to the third order in parameter $\alpha = a_b/a_c$ and averaged over both mean longitudes l_j , $j = b, c$. The relevant parameters of the secular theory are defined through the momenta conjugated to the mean longitudes and arguments of periastron $g_j = \omega_j$:

$$\begin{aligned} L_b &= \frac{m_\star m_b}{m_\star + m_b} \sqrt{G(m_\star + m_b)a_b}, \\ L_c &= \frac{(m_\star + m_b)m_c}{m_\star + m_b + m_c} \sqrt{G(m_\star + m_b + m_c)a_c}, \\ G_j &= L_j \sqrt{1 - e_j^2}, \end{aligned} \tag{1}$$

where m_\star is the mass of the parent star. The momenta are, respectively, the magnitude of the maximum possible angular momentum (for circular orbits) and the magnitude of the angular momentum. The sum of the remaining two momenta, $H_j = G_j \cos i_j$, is the z -component of the angular momentum of the system conjugate to the longitudes of the ascending node $h_j = \Omega_j$. Let us note, that this formulation is valid in the general case of an inclined system. In coplanar configurations ω_j are undefined but then the longitudes of periastron ϖ_j take over their role. In the averaged system, l_j are absent in the Hamiltonian and L_j are constants of motion. Because the octopole-level Hamiltonian depends only on the combination $\varpi_b - \varpi_c$, it

turns out that the total angular momentum $G_b + G_c$ is also the integral of motion in the averaged system. This reduces the coplanar dynamics to 1 degree of freedom, with e_b or e_c , and θ as the relevant phase-space variables. The authors found that for the same constants:

$$\beta = \frac{5(m_* - m_b)}{4(m_* + m_b)}\alpha,$$

$\lambda = L_b/L_c$, the same initial e_b, e_c and $\theta = \varpi_b - \varpi_c$ the averaged equations of motion describe the same trajectories in the phase-space diagram of $e_{b,c}(\theta)$. For planetary masses much smaller than the central body, these trajectories and the amplitudes of eccentricity oscillations should be independent of the inclination of the system. Further, by introducing the parameter $\gamma = (G_b + G_c)/(L_b + L_c)$ which describes the non-dimensional total angular momentum of the system, one defines the critical value of λ ,

$$\lambda_{\text{crit}} = \frac{2\gamma^2}{5 - 3\gamma^2}.$$

According to the equations of motion in the averaged system, if $\lambda \simeq \lambda_{\text{crit}}$ then libration of θ is almost certain with possibly large amplitude variations of both eccentricities. In general, the librations can take place about two libration centers, 0° or 180° . Using the fits published in Fischer et al. (2003), the authors found that indeed, for HD 12661 system, $\lambda \simeq \lambda_{\text{crit}}$ and they identified an extended libration island of the SAR with the apsides antialigned in the exact resonance.

Following Lee & Peale (2003), we examined the ICs for the HD 169830 and HD 12661 systems by calculating these phase-space diagrams numerically. To obtain such diagrams, we fixed the constant level of the total angular momentum corresponding to the nominal IC and the phase curves were computed for varied e_c (e_b was calculated from the total momentum integral, the formula 1). The time of integrations was the same as for the derivation of the 2-dimensional stability maps. The results are shown in Figure 11. For both ICI of the HD 169830 and IC0 of the HD 12661 systems, the phase space is occupied by two large libration islands about $\theta = 0^\circ$ and $\theta = 180^\circ$ which is consistent with the secular theory. For the ICI of the HD 169830 system, $\lambda = 0.644$ and $\lambda_{\text{crit}} = 0.9$, so these parameters substantially differ. However, Fig. 11 shows that the occurrence of a libration mode still appears more likely than the θ rotations. For the IC0 of the HD 12661, $\lambda = 0.75$ is closer to its critical value $\lambda_{\text{crit}} = 0.87$, and indeed, the the resonance island is more extended.

The configuration corresponding to ICI of the HD 169830 system is localized almost on the border of the island of the antialigned SAR. This border is a separatrix and if the initial $e_c \simeq 0$, the semi-amplitude of θ librations approaches 90° as the system enters the vicinity of the separatrix. In the resonance island, the librations are about the libration center $\theta = 180^\circ$. The diagram also helps us to understand the large amplitudes of the eccentricities. Qualitatively, one obtains the same picture for the HD 12661 system. For the ICII of the HD 169830 system, we have $\lambda = 0.97$ and $\lambda_{\text{crit}} = 0.77$. In this case the nominal HD 169830 system lies in an extended area of θ -rotations seen in Fig. 11.

The octupole theory allows us to quickly examine the extent of the SAR in the space of the orbital parameters. Because the elements of the inner planet are well determined, the overall picture of the HD 169830 dynamics depends mostly on the not too well constrained parameters of the outer planet. Assuming that strong mean motion resonances are absent, the secular dynamics can be investigated in detail through solving Equations (1)–(4) of Lee & Peale (2003). These equations describe the secular time-evolution of $e_{b,c}$ and $\varpi_{b,c}$. Unfortunately, there seems to be no explicit, analytical solution to these equations. Also a construction of a simple SAR criterion, like the one developed by Laughlin et al. (2002) or Ji et al. (2003) in the framework of the Laplace-Lagrange secular theory, does not appear to be possible, either. However, these

equations are very simple for a numerical treatment and their direct integration is rapid, hundreds times faster than the N -body integrations. The SAR can be detected in the parameter space by looking for the maximal deviations of θ from the given libration center 0° or 180° . It is the same method of detecting the SAR as the one applied in the full N -body integrations but here it is well justified because according to the generic secular dynamics, the SAR appears about two libration centers. Assuming that the integration time covers at least one secular period (so as it is not too short), we can easily detect the librations or rotations of the critical argument θ .

Using this approach, we computed a number of the SAR-maps in the (a_c, e_c) and (e_b, e_c) domains for the initial conditions ICI, ICII and IC0. In order to directly compare the results, the ranges of the parameters were the same as for the numerical maps. The results are shown in Fig. 12. Generally, they agree in the regions corresponding to small eccentricities, for which both the shape of these regions and the semi-amplitude of librations are well reproduced by the secular theory. However, we can also find significant discrepancies between the analytical and numerical estimations. For example for ICII, in the (a_c, e_c) -plane one can find islands of the SAR which are absent in the map computed by solving the secular equations. The differences are also apparent in the (e_b, e_c) plane for all examined IC's. In these cases, the results agree only in the regions of relatively small e_c .

In order to understand these differences, we compared the (e_c, θ) diagrams obtained by the direct numerical integrations and by solving the secular equations. The tests were performed for: (a) ICI in which we changed eccentricities to $e_b = 0.3, e_c = 0.3$, (b) ICII with $a_c = 3.51, e_c = 0.47$ (see bottom-middle panel in Fig. 7 corresponding to the center of the 9:1 MMR) (c) ICII with $(e_b = 0.47, e_c = 0.47)$ (corresponding to the island in the bottom middle panel in Fig. 8). The results are presented in Fig. 13. In all these cases, the full dynamics seems to be only roughly described by the secular approximation. The disagreement is obviously expected in the case (b) since the assumptions of the secular theory are violated (an MMR is present). In other two examples, the differences are most likely due to significant mutual interactions caused by large eccentricities resulting in deformations of the phase-space curves (case a) or a chaotic evolution (case c). Clearly the secular theory should be applied with caution.

7. Conclusions

In this paper we carry out a dynamical analysis of the recently discovered 2-planetary exosystem around HD 12661. According to the preliminary initial orbital parameters announced by the Geneva Extrasolar Planet Search team (orbital solution ICI), this system resembled the other known planetary hierarchical exosystem HD 12661 and the HD 160691. The recently updated orbital solution (ICII) has been changed in a significant way and the close similarity of the HD 169830 and HD 12661 systems is not so apparent anymore.

The exosystems around HD 12661, HD 160691 and HD 169830 belong to a class of the hierarchical planetary systems. They are characterized by a relatively small ratio of the semi-major axes, $\simeq 0.1 - 0.3$. Their dynamics should be analyzed in the Jacobi orbital elements (Lee & Peale 2003; Goździewski et al. 2003). The commonly used astrometric elements may lead to small shifts of the positions of the orbital resonances and to differences in the evolution of the osculating orbital elements. Following these papers we used the two orbital fits published by the discovery team but we recomputed the semi-major axes and masses of the companions. The current ICII was verified by our independent analysis of the approximate RV measurements which we obtained by digitizing a figure with the synthetic best-fit RV curve and the real

observational points. Such an "approach" to obtain the "observations" was forced by the lack of access to the real data. Since the $(\chi_\nu^2)^{1/2}$ function will typically have many local minima, we cannot be sure that a solution is the proper one without a global $(\chi_\nu^2)^{1/2}$ analysis. As demonstrated on the solution ICI and ICII of the HD 169830 system, the difference between the global and a local minimum may lead to enormous differences in the overall dynamical picture of the system. Obviously, the digitization cannot provide very accurate moments of the observations, nevertheless such "data" describe the overall shape of the real RV measurements quite precisely and make it possible to obtain some insight into the quality of the best fit solution by the discovery team. Using the genetic algorithm to find the global minimum of $(\chi_\nu^2)^{1/2}$ and describing the measurements with the 2-planet Keplerian and Newtonian models, we found almost the same orbital elements of the inner planet as these reported by the discovery team and very similar elements for the outer companion. The application of the 2-Keplerian and N -body models produced the same value of $(\chi_\nu^2)^{1/2}$ and similar orbital solutions. It demonstrates the absence of strong interactions between the planets. It also favors the solution with a large separation between the companions rather than the previously announced configuration. Apparently, the first orbital solution was just a local minimum of the $(\chi_\nu^2)^{1/2}$ function.

The two orbital solutions have different dynamical features. The ICI solution is close to an unstable 13:2 MMR and lies between 6:1 and 7:1 MMRs. The exosystem corresponding to ICII is located between 9:1 and 10:1 MMRs. Both configurations appear to be stable on the Gyr time scale as demonstrated by our long-term integrations, the fast indicator analysis and the secular octupole-level theory. In the phase space, both ICs are lie in the wide regions of stable motions in spite of large variations of the eccentricities (up to 0.5). Obviously, these conclusions may changed in the future as the time-span of the current RV measurements is shorter than the period of the outer planet. Moreover, the moderately constrained orbital elements of the outer planet do not allow us to exclude a proximity of the system to an unstable low-order resonance. The main dynamical difference between the two ICs is the SAR with the apsidal lines antialigned in the exact resonance. It is present for ICI in the wide ranges of the orbital parameters while for the ICII it seems to be ruled out. In the first case, the HD 169830 would be very similar to the hierarchical resonant systems. In this "class" we can find the discussed HD 12661 and possibly the HD 160691 exosystem. The HD 37124 (Butler et al. 2003) system could also be a member of this group. However, in the HD 37124 system the apsides are most likely aligned (Ji et al. 2003). If the two outer planets are taken into consideration, the ν Andromedae (Butler et al. 1999) system could also be assigned to this group (Chiang & Murray 2002). However, the new orbital solution ICII favors the proximity of the HD 169830 system to the HPS with the outer, very massive (possibly sub-stellar) companion like the HD 38529 (Fischer et al. 2003), HD 74156⁹ and HD 168443 (Marcy et al. 2001; Udry et al. 2002) systems. In these systems, the stability is maintained thanks to a relatively large separation of the companions. Nevertheless, due to very large masses involved and large amplitudes of the eccentricity variations, the mechanism providing the stability is puzzling.

The results of the numerical analysis of the orbital evolution and stability can be compared with the predictions by the secular octupole-level theory of Lee & Peale (2003). The results of both approaches are in accord for moderately low eccentricities of the outer planet. The discrepancies appear if both eccentricities are large in the regions of the phase space close to the MMRs and in the chaotic zones. It seems that although the secular theory makes it possible to explain the main features of the HD 169830 -like systems, the direct integrations are still necessary to understand the dynamics in detail.

For a better grasp on the dynamical picture of the HD 169830 system, we need to wait for some time, ideally until the observations cover a few orbital periods of the outer companion. Since the orbital elements

⁹<http://obswww.unige.ch/udry/planet/hd74156.html>

of the inner companions are similar in the HD 169830 and HD 12661 systems and are already determined with high accuracy, there is still a chance that our preliminary hypothesis that the two planetary systems are dynamically related is plausible.

8. Acknowledgments

We thank Man Hoi Lee for a discussion about the Jacobi elements and Ji Janghai for useful remarks. This work is supported by the Polish Committee for Scientific Research, Grant No. 2P03D 001 22. M. K. is a Michelson Postdoctoral Fellow.

REFERENCES

- Butler, R. P., Marcy, G. W., Fischer, D. A., Brown, T. M., Contos, A. R., Korzennik, S. G., Nisenson, P., & Noyes, R. W. 1999, *ApJ*, 526, 916, 1999ApJ...526..916B
- Butler, R. P., Marcy, G. W., Vogt, S. S., Fischer, D. A., Henry, G. W., Laughlin, G., & Wright, J. T. 2003, *ApJ*, 582, 455
- Charbonneau, P. 1995, *ApJS*, 101, 309
- Chiang, E. I. & Murray, N. 2002, *ApJ*, 576, 473
- Chiang, E. I., Tabachnik, S., & Tremaine S. 2001, *AJ*, 122, 1607
- Cincotta, P. M. & Simó, C. 2000, *A&AS*, 147, 205
- Fischer, D. A., Marcy, G. W., Butler, R. P., Vogt, S. S., Henry, G. W., Pourbaix, D., Walp, B., Misch, A. A., & Wright, J. T. 2003, *ApJ*, 586, 1394
- Goździewski. 2003, *A&A*, 398, 1151
- Goździewski, K., Konacki, M., & Maciejewski, A. J. 2003, *ApJ*, 594
- Goździewski, K. & Maciejewski, A. J. 2003, *ApJ*, 586, L153
- Goździewski, K. 2003, *A&A*, 398, 315
- Goździewski, K., Bois, E., Maciejewski, A., & Kiseleva-Eggleton, L. 2001, *A&A*, 378, 569
- Hairer, E. & Wanner, G. 1995, [http://www.unige.ch/math/folks/haierer/](http://www.unige.ch/math/folks/haier/)
- Holman, M., Touma, J., & Tremaine, S. 1997, *Nature*, 386, 254
- Ji, J., Liu, L., Kinoshita, H., Zhou, J., Nakai, H., & Li, G. 2003, *ApJ*, 591, L57
- Jones, H. R. A., Paul Butler, R., Marcy, G. W., Tinney, C. G., Penny, A. J., McCarthy, C., & Carter, B. D. 2002, *MNRAS*, 337, 1170
- Kozai, Y. 1962, *AJ*, 67, 591+
- Laskar, J. 1993, *Celest. Mech. & Dyn. Astr.*, 56, 191

- Laughlin, G., Chambers, J., & Fischer, D. 2002, *ApJ*, 579, 455
- Laughlin, G. & Chambers, J. E. 2001, *ApJ*, 551, L109
- Lee, M. H. & Peale, S. J. 2003, *ApJ*, 592, 1201
- Levison, H. F. & Duncan, M. J. 1994, *Icarus*, 108, 18
- Marcy, G., Butler, R., Fischer, D., Vogt, S., Lissauer, J., & Rivera, E. 2001, *ApJ*, 556, 296
- Mayor, M., Udry, S., Naef, D., Pepe, F., Queloz, D., Santos, N. C., & Burnet, M. 2003, *A&A*, astro-ph/0310316
- Press, W. H., Teukolsky, S. A., Vetterling, W. T., & Flannery, B. P. 1992, *Numerical Recipes in C. The Art of Scientific Computing* (Cambridge Univ. Press)
- Robutel, P. & Laskar, J. 2001, *Icarus*, 152, 4
- Sidlichovsky, M. & Nesvorny, D. 1997, *Celestial Mechanics and Dynamical Astronomy*, 65, 137
- Udry, S., Mayor, M., Naef, D., Pepe, F., Queloz, D., Santos, N. C., & Burnet, M. 2002, *A&A*, 390, 267

Fig. 1.— The orbital evolution (expressed in the osculating orbital elements of Jacobi) of the HD 169830 system for the nominal ICI given in Table 1. Panels (a,b) show changes of the semi-major axes. Panel (c) is for the eccentricities. Panel (d) shows the critical argument of the apsidal resonance $\theta = \varpi_b - \varpi_c$. Panel (e) is for MEGNO as a function of time, $Y(t)$, and panel (f) is for its mean value $\langle Y \rangle$.

Fig. 2.— The orbital evolution of the HD 169830 planetary system for the ICII given in Table 1. The description of the panels is the same as in the previous figure.

Fig. 3.— The orbital evolution of the HD12661 planetary system for the IC given in Table 3. The description of the panels is the same as in the previous figure.

Fig. 4.— The digitized RV data of the HD 169830 system and the synthetic RV curves corresponding to the best fits found from this paper. The thicker line is for the N -body model. The orbital parameters of the solutions are given in Table 2.

Fig. 5.— Confidence intervals corresponding to 1σ , 2σ and 3σ levels of $(\chi_\nu^2)^{1/2}$ obtained for the best N -body fit to the digitized RV data. The fit is given in Table 2.

Fig. 6.— Scans of MEGNO (upper graphs in every panel) and the diffusion rate of the proper mean motion of the outer planet (lower graphs labeled by $\log \sigma_c$) for the ICI of the HD 169830 system (the top panel) ICII of the HD 169830 system (the middle panel) and for the HD 12661 system (the bottom panel) over the semi-major axis of the outer planet (in AU). The resolution of the plot is $\simeq 3 \cdot 10^{-4}$ AU. Labels mark the positions of the strongest mean motion resonances (up to the order about 20) as they have been identified by the FMA. The nominal values of a_c are marked with big dots.

Fig. 7.— The stability of the HD 169830 system in the (a_c, e_c) -plane. The left panels are for MEGNO. The middle panels give an estimate of the semi-amplitude of the apsidal librations, θ^{\max} , about the line of apsides antialignment (note that the white areas are for $\theta^{\max} \geq 90^\circ$). The right panels show the maximal eccentricity of the inner planet. The data grid has the resolution of $0.006\text{AU} \times 0.005$. The top row is for the ICI, the bottom row is for the ICII.

Fig. 8.— The stability of the HD 169830 system in the plane of the eccentricities. The left panels are for MEGNO. The middle panels give an estimate of the semi-amplitude of the apsidal librations, θ^{\max} , about 180° . Note that the white areas are for $\theta^{\max} \geq 90^\circ$. The right panels show the maximal eccentricity of the inner planet. The data grid has the resolution of 100×100 points. The top row is for the ICI, the bottom row is for the ICII.

Fig. 9.— The stability map of the HD 169830 system when the relative inclination of the orbits and the absolute inclination i are varied. The left panels are for MEGNO. The middle panels show the semi-amplitude of librations of θ about 180° . The white areas are for $\theta^{\max} \geq 90^\circ$. The right panels show the maximal eccentricity of the inner planet. The data grid has the resolution of $3^\circ \times 1^\circ$. The top row is for the ICI, the bottom row is for the ICII.

Fig. 10.— The evolution of the inclination and eccentricities in the planetary configuration corresponding to ICII when the initial relative inclination of orbits has been changed to 80° . The left panel is for the inner planet and the right panel is for the outer companion. The bottom plots are for the eccentricities magnified by 100.

Fig. 11.— The phase-space diagrams at the same level of the total angular momentum. The left column is for the ICI, the middle column is for the HD 12661 system, the right column is for the ICII. The nominal ICs are marked with a big dot. The phase-space trajectories have been computed for the initial $\theta = 0^\circ$ and for $\theta = 180^\circ$; e_c varies while e_b is determined from the integral of the total angular momentum. Other orbital parameters are fixed at their nominal values.

Fig. 12.— The semi-amplitude of the SAR about the libration center 180° in the planes of semi-major axes and eccentricities as predicted by the secular octupole theory. The left column is for the ICI, the middle column is for the ICII of the HD 169830 system and the right column is for the IC0 of the HD 12661 system. The white areas are for $\theta^{\max} \geq 90^\circ$.

Fig. 13.— The comparison of the phase-space diagrams at the same level of the total angular momentum obtained from the numerical integration of the full equations of motion (top row) and derived from the secular-octupole theory (bottom row). The initial conditions correspond to the modified ICI and ICII (see text for explanation). The modified initial conditions are marked with big dots. They correspond to the coordinates marked with (a), (b) and (c) in Fig. 7, 8, respectively.

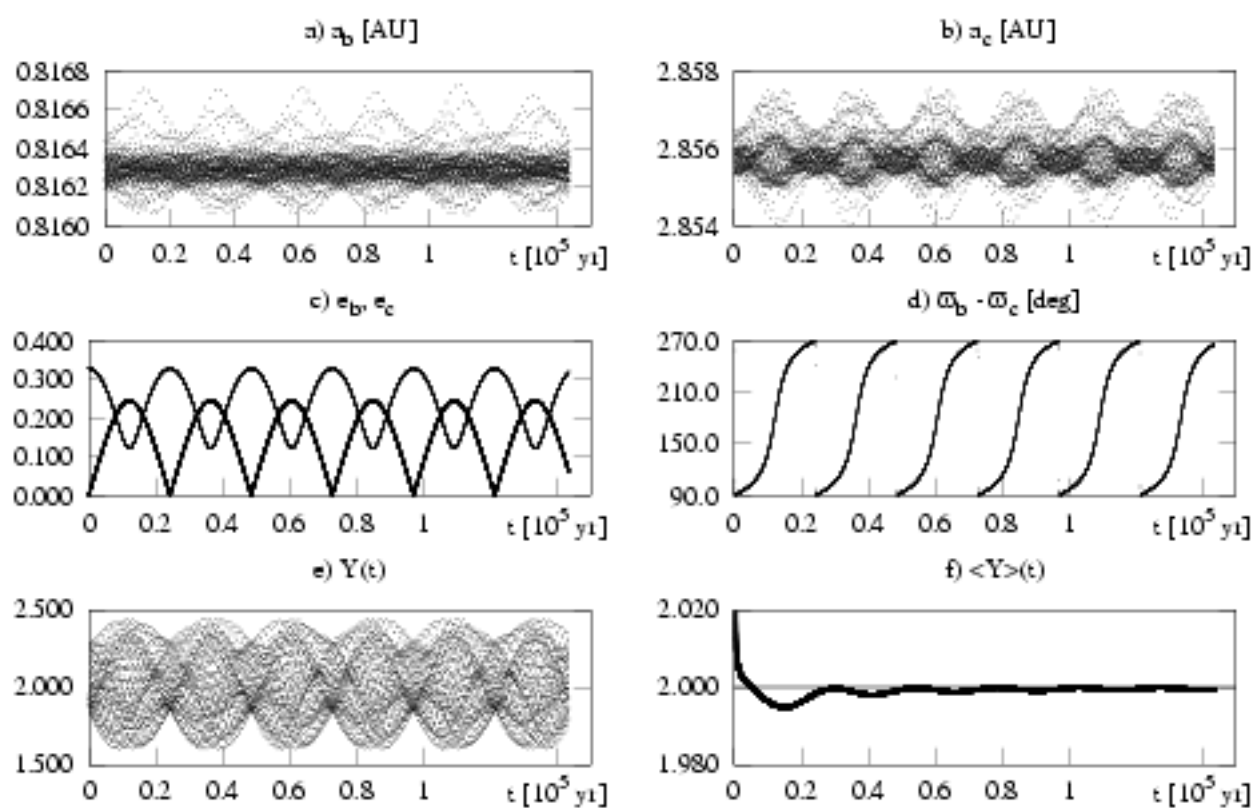


Fig. 1.—

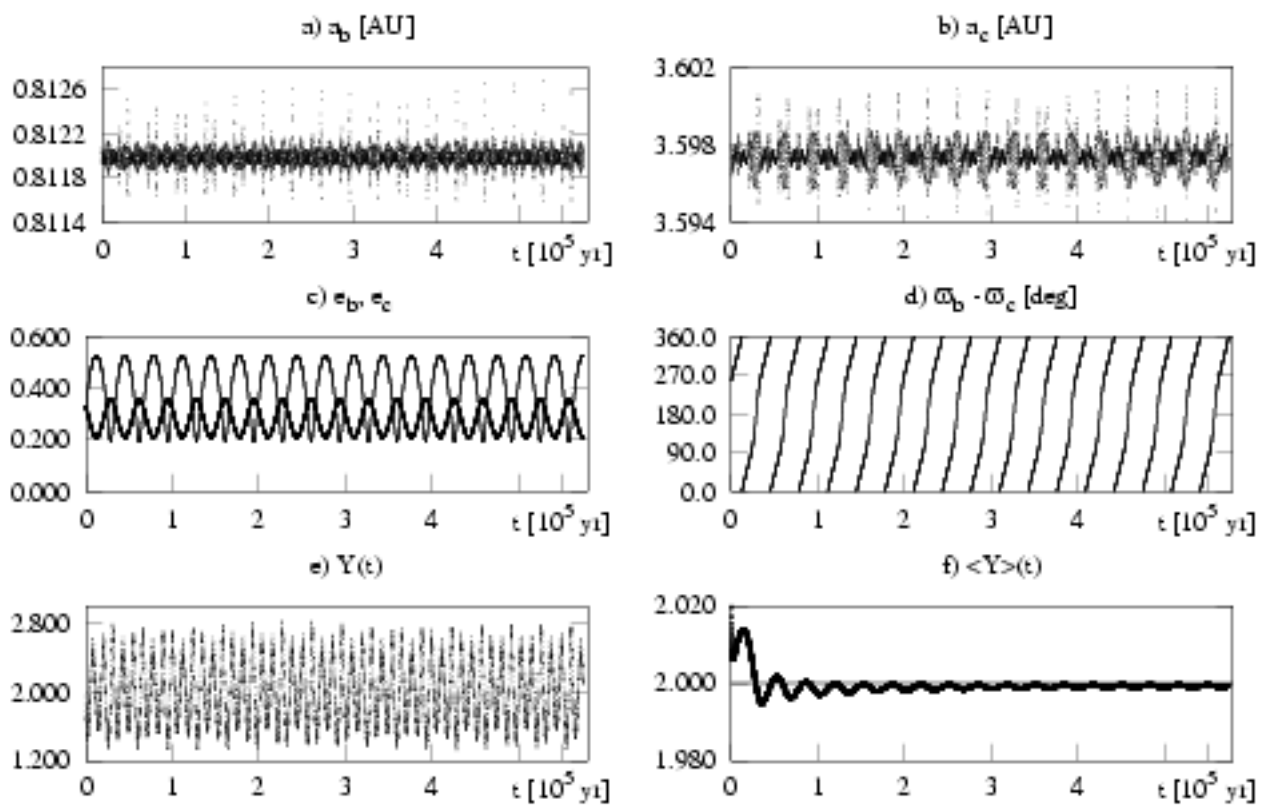


Fig. 2.—

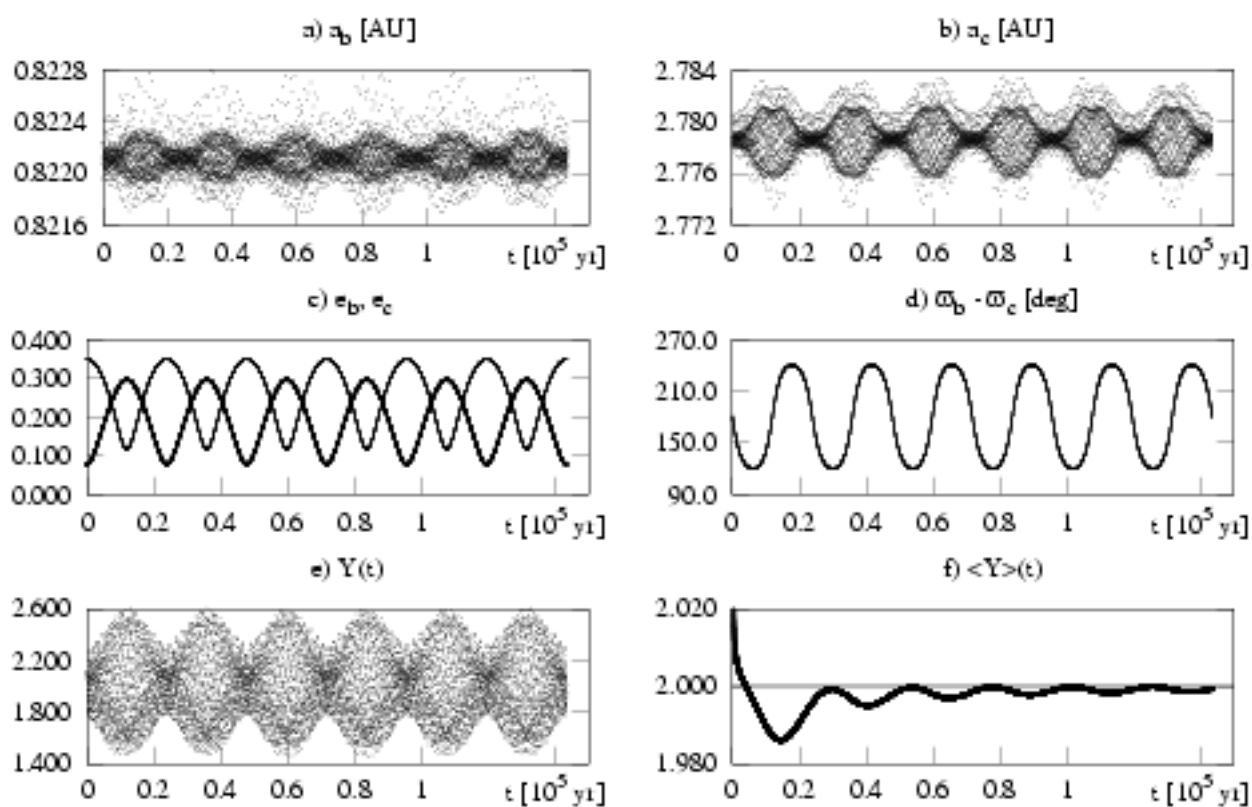


Fig. 3.—

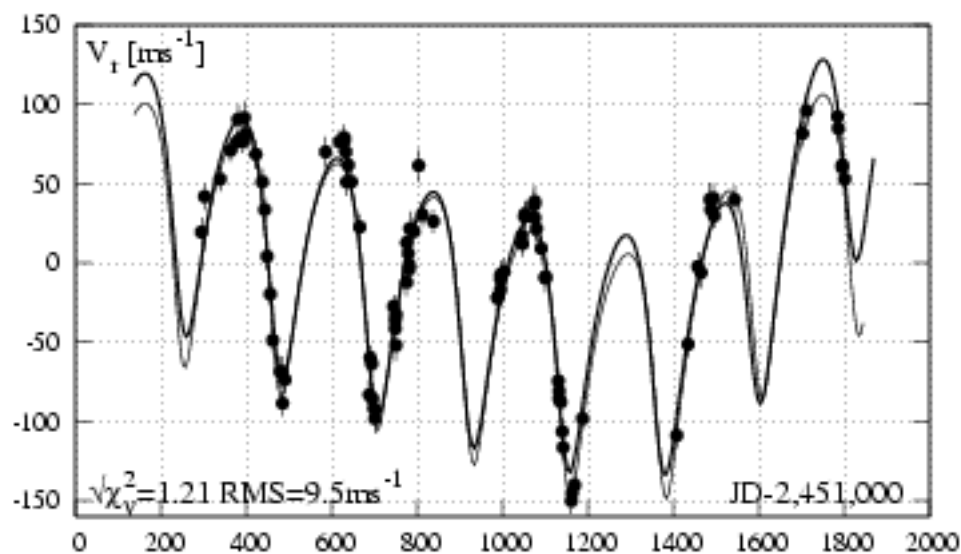


Fig. 4.—

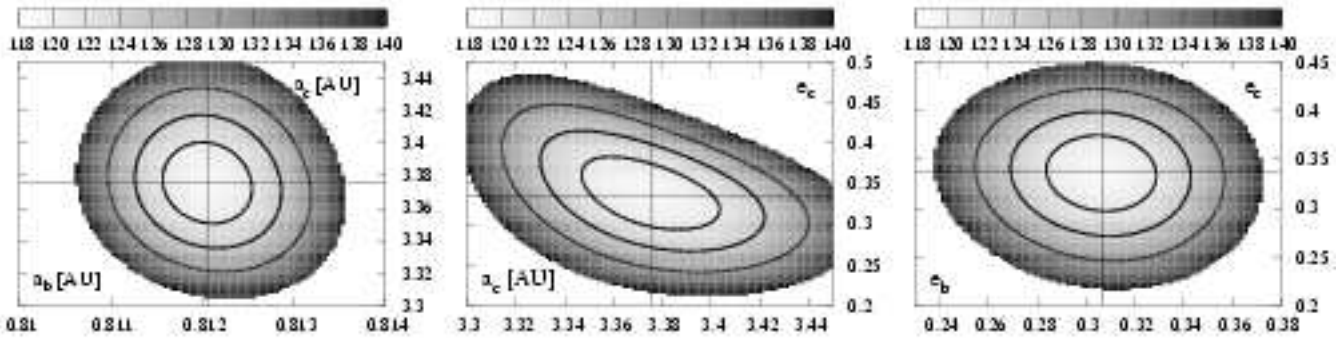


Fig. 5.—

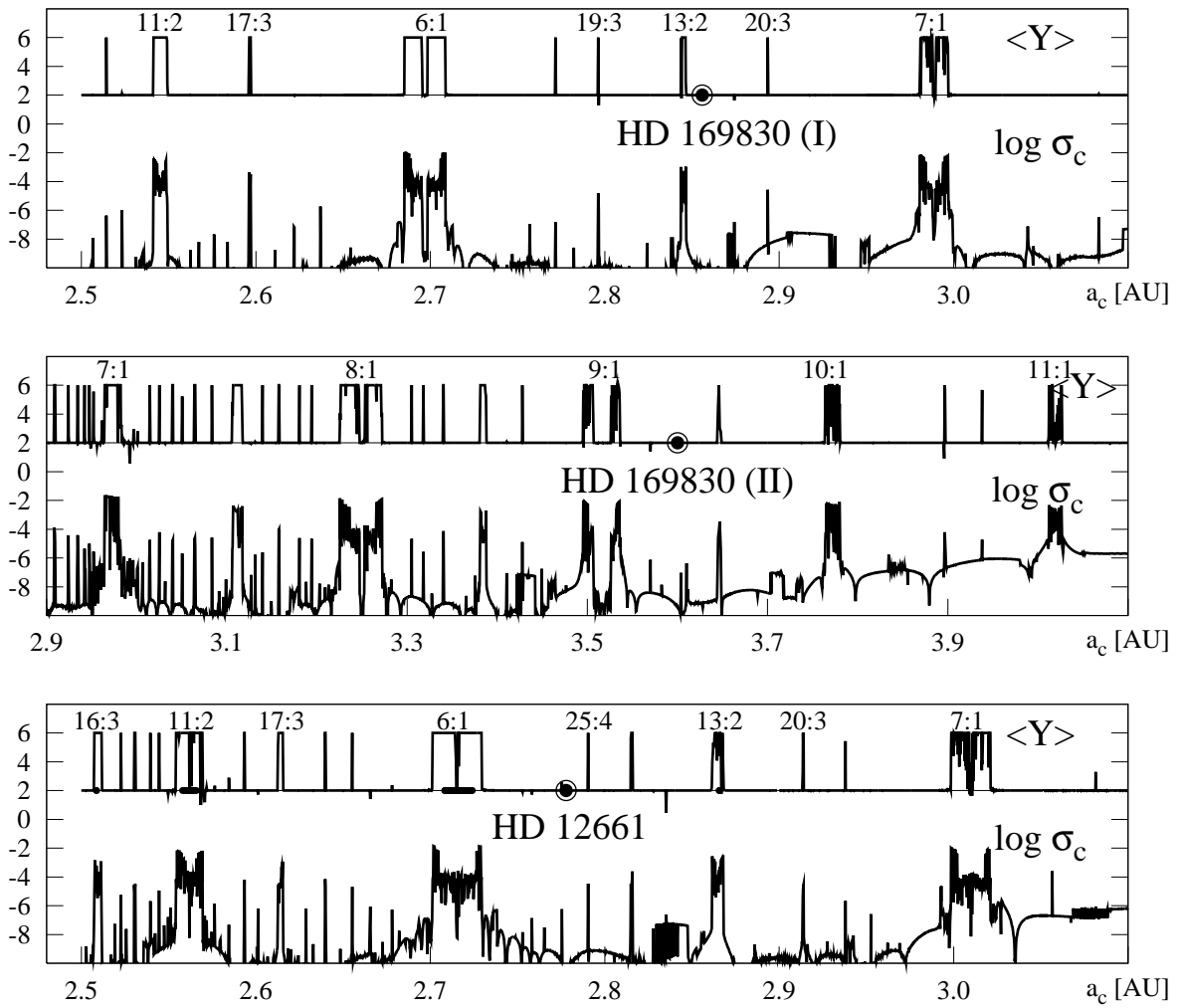


Fig. 6.—

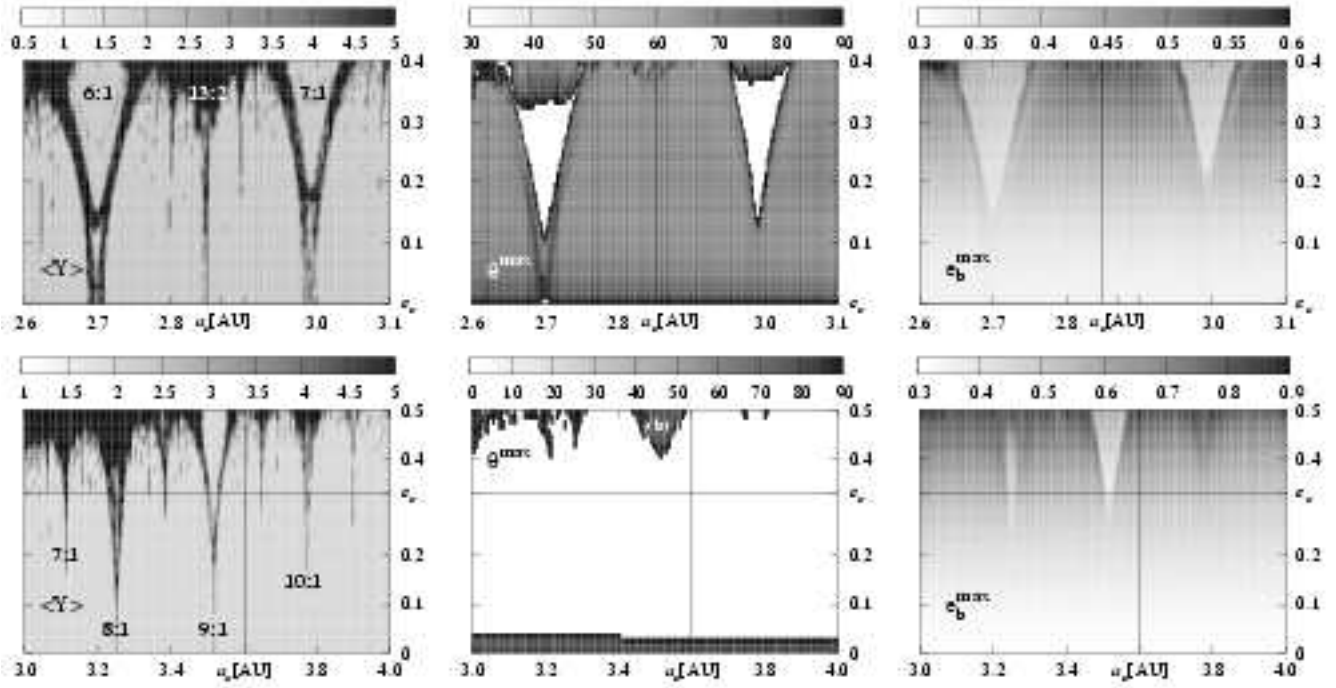


Fig. 7.—

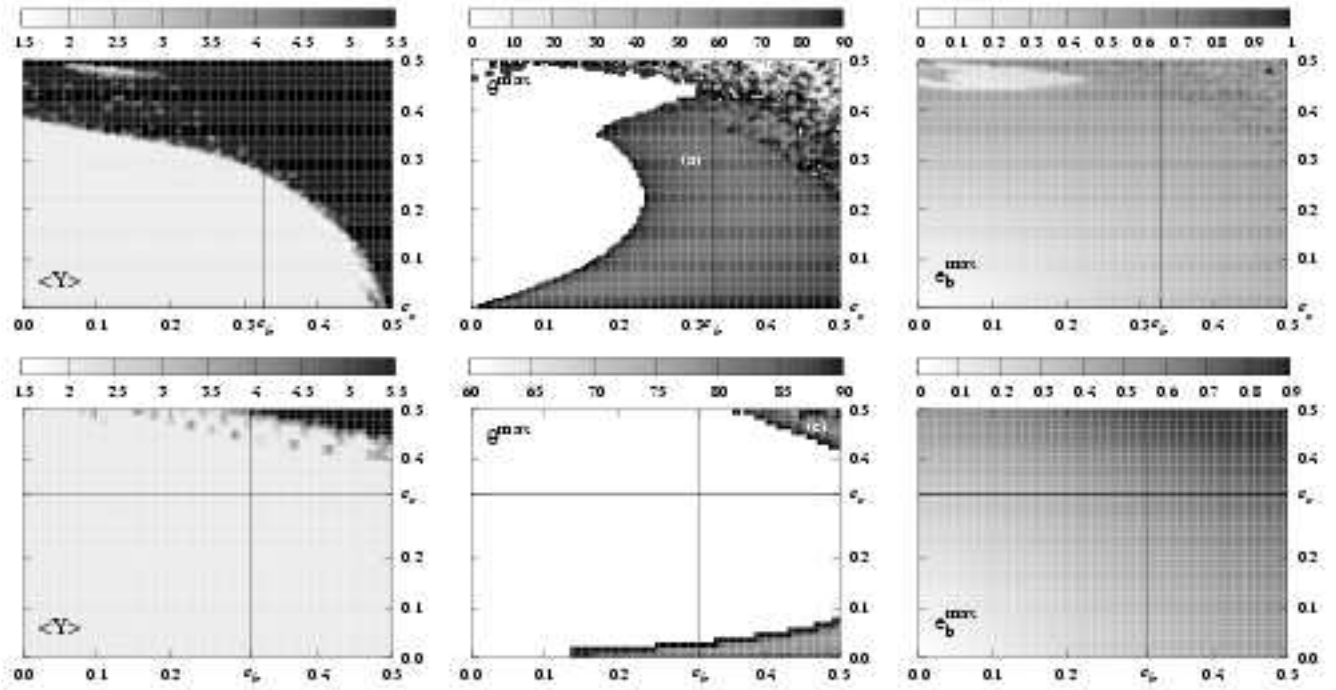


Fig. 8.—

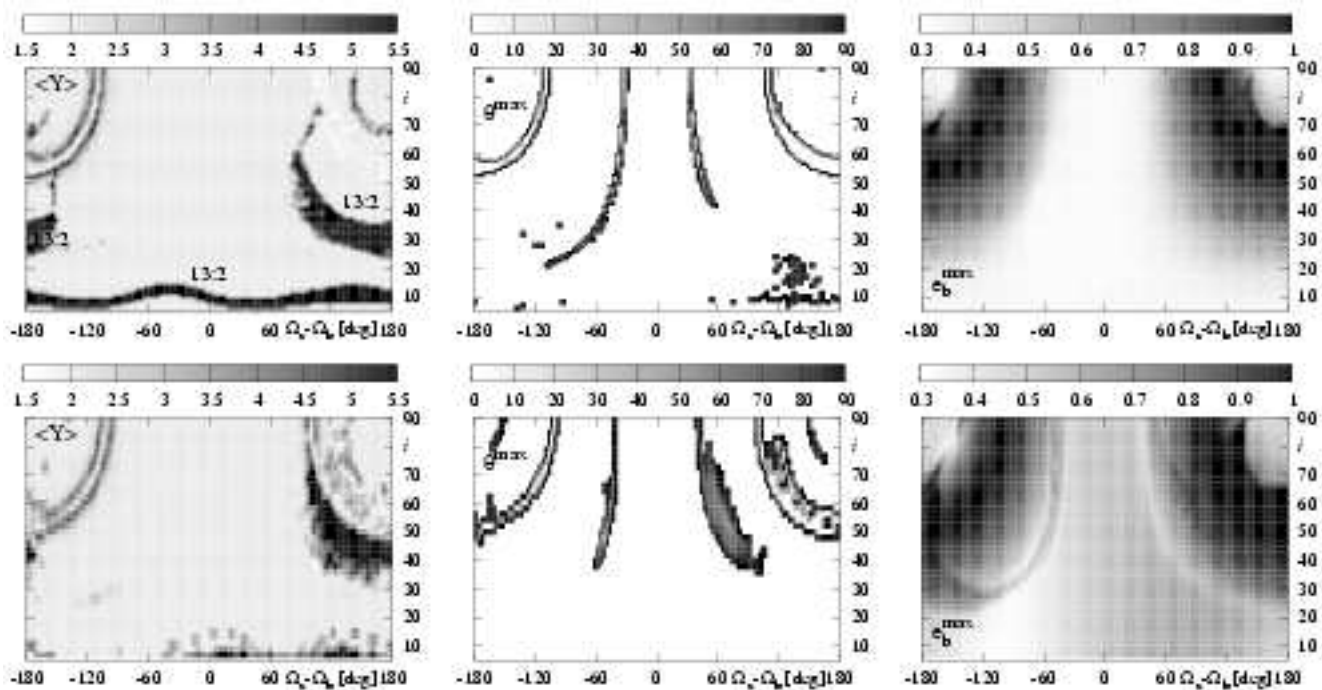


Fig. 9.—

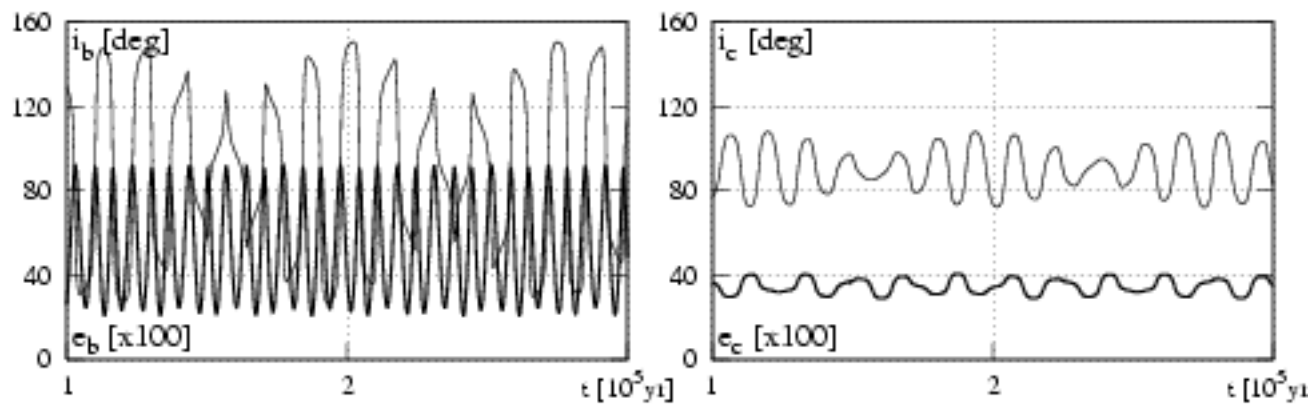


Fig. 10.—

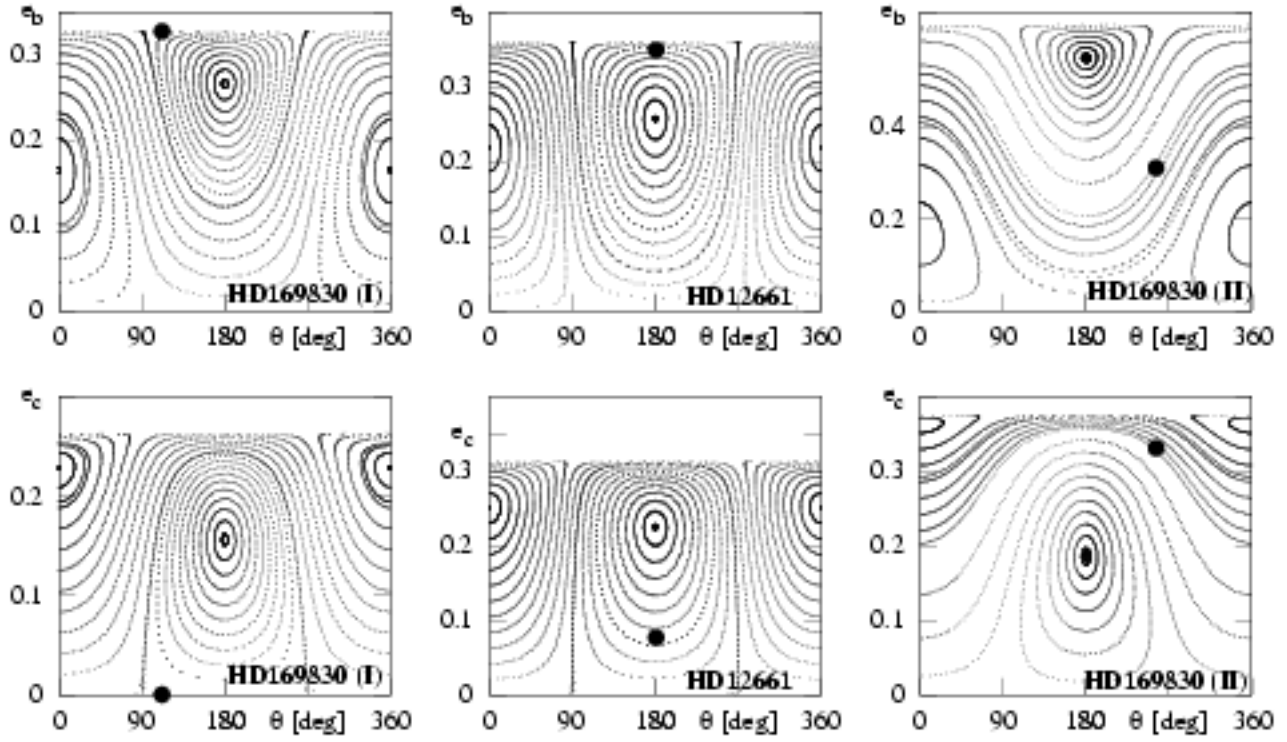


Fig. 11.—

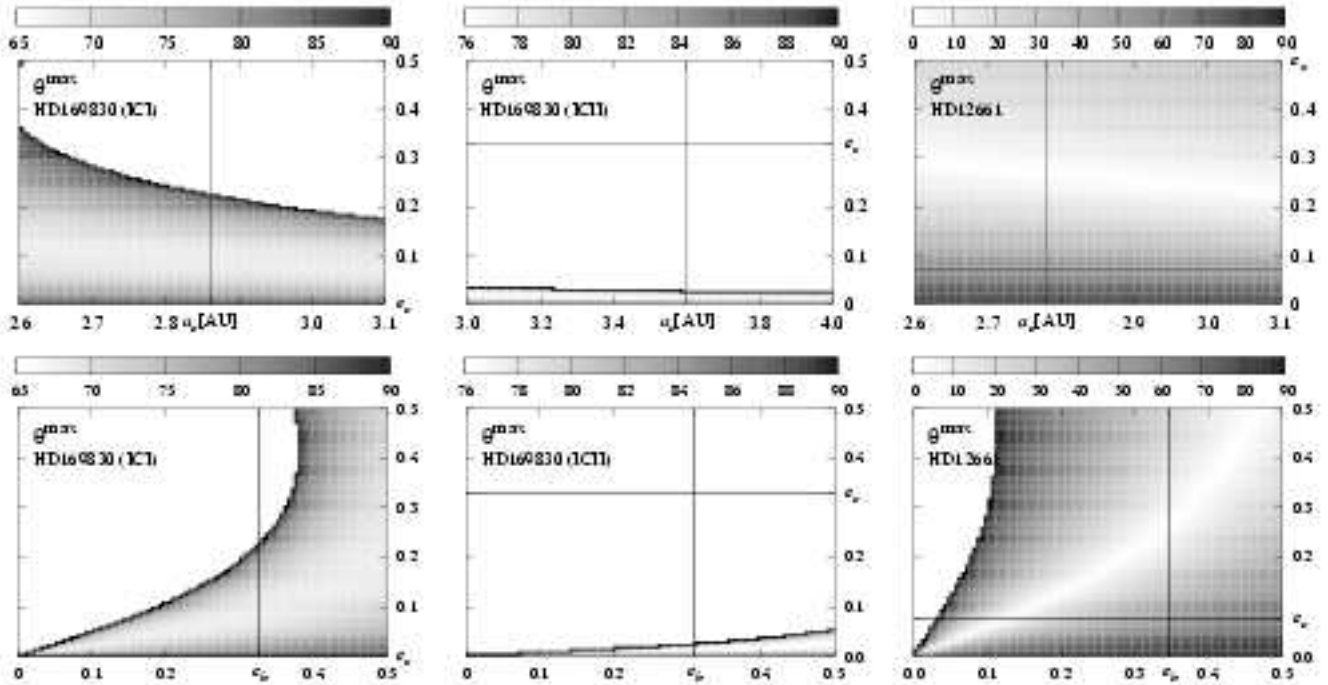


Fig. 12.—

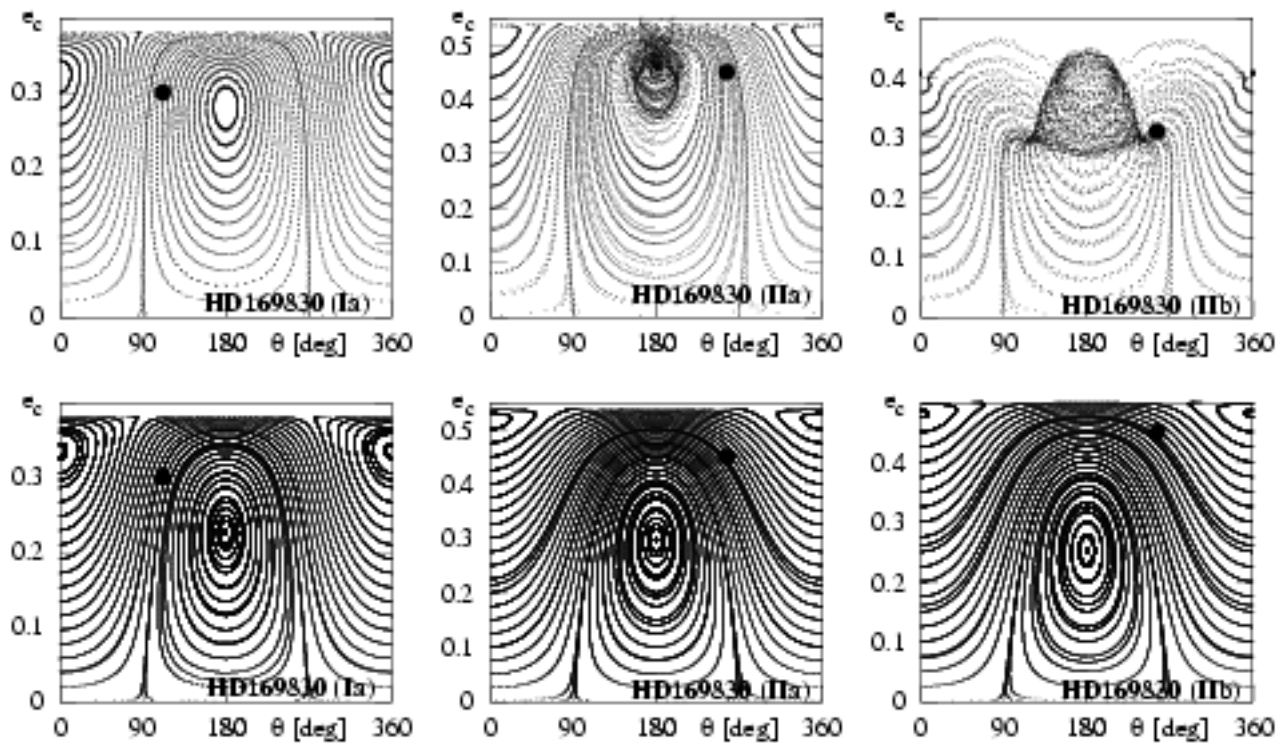


Fig. 13.—

Table 1: Jacobi orbital parameters of the HD 169830 system from http://obswww.unige.ch/udry/planet/hd169830_syst.html (updated on August, 28, 2003; the ICII solution). The first version of the fit (dated 28 June, 2003; the ICI solution) is given in the parentheses. The mass of the central star is equal to $1.4 M_{\odot}$.

| Jacobi orbital parameter | Planet b | Planet c |
|------------------------------|----------------------------|------------------------|
| $m_2 \sin i$ [M_J] | 2.88 (3.03) | 4.05 (2.51) |
| a [AU] | 0.811 (0.816) | 2.856 (3.598) |
| P [d] | 225.62 ± 0.22 (227.43) | 2102 ± 264 (1487) |
| e | 0.31 ± 0.01 (0.327) | 0.33 ± 0.02 (0.0) |
| ω [deg] | 148 ± 2 (156.1) | 252 ± 8 (44.0) |
| T_p [JD-2,400,000] | 51923 ± 1 (51472.43) | 52516 ± 25 (50101) |
| $M(T_b)$ [deg] | 0.00 | 258.4 (332.2) |

Table 2: Jacobi orbital parameters of the HD 169830 system based on the digitized figure from http://obswww.unige.ch/udry/planet/hd169830_syst.html (the version updated on August, 28, 2003). Numbers without parentheses are for Jacobi elements of the 2-Keplerian solution. Values in parentheses are for the osculating, Jacobi elements from the N -body, self-consistent fit given for the date of the first digitized observation (JD=2,451,294.97). The mass of the central star is equal to $1.4 M_{\odot}$.

| Orbital parameter | Planet b | Planet c |
|------------------------------|---------------|---------------|
| $m_2 \sin i$ [M_J] | 2.86 (2.85) | 3.88 (3.84) |
| a [AU] | 0.812 (0.812) | 3.41 (3.38) |
| P [d] | 225.62 | 1939.4 |
| e | 0.307 (0.307) | 0.334 (0.336) |
| ω [deg] | 148.6 (148.8) | 260.1 (260.5) |
| T_p [JD-2,400,000] | 51922.5 | 52533 |
| M [deg] | 0.0 (78.9) | 204.7 (128.1) |
| $(\chi^2)^{1/2}$ | 1.21 (1.21) | |
| RMS [m/s] | 10 (9.5) | |
| V_0 [m/s] | 3.35 (6.3) | |

Table 3: Orbital parameters of the HD 12661 system from Goździewski & Maciejewski (2003) for the epoch of the first observation (JD=2,450,831.608). The mass of the central star is equal to $1.08 M_{\odot}$. The orbital periods come from the FMA as reciprocals of the proper mean motion frequencies.

| Orbital parameter | Planet b | Planet c |
|------------------------------|----------|----------|
| $m_2 \sin i$ [M_J] | 2.33 | 1.69 |
| a [AU] | 0.82 | 2.78 |
| P [d] | 263 | 1632 |
| e | 0.349 | 0.076 |
| ω [deg] | 115.2 | 294.4 |
| M [deg] | 129.37 | 352.9 |